26 October 2001

ELSEVIER

Chemical Physics Letters 347 (2001) 304–310

CHEMICAL PHYSICS LETTERS

www.elsevier.com/locate/cplett

Ultrafast and long-lived photoinduced charge separation in MEH-PPV/nanoporous semiconductor thin film composites

Neil A. Anderson [a], Encai Hao [a], Xin Ai [a], Gary Hastings [b], Tianquan Lian [a,*]

[a] *Department of Chemistry, Emory University, Atlanta, GA 30322, USA*
[b] *Department of Physics and Astronomy, Georgia State University, Atlanta, GA 30303, USA*

Received 18 May 2001; in final form 18 July 2001

Abstract

Photoinduced charge separation and recombination dynamics were investigated in composite materials of conjugated polymer deposited on nanocrystalline metal oxide thin film. Using femtosecond IR transient absorption spectroscopy, the electron transfer from the excited state of poly[2-methoxy-5-(2-ethyl-hexyloxy)-(phenylene vinylene)] (MEH-PPV) to SnO_2 and TiO_2 nanoporous thin films is shown to occur with timescales of 800 and <100 fs, respectively. Negligible carrier recombination is observed for MEH-PPV/SnO_2 within 1 ns. Microsecond charge recombination dynamics were measured using step-scan FTIR. Long-lived charge separation is observed in both systems, persisting for microseconds to seconds. © 2001 Elsevier Science B.V. All rights reserved.

1. Introduction

Recently, composite materials of inorganic semiconductor nanoparticles and conjugated polymers have attracted much interest as photovoltaic materials. These materials are attractive because of their potential to combine the unique properties of semiconductor nanoparticles [1] and conjugated polymers [2]. Photoinduced electron transfer has been demonstrated in composites of conjugated polymer/C_{60} [3], conjugated polymer/CdS and CdSe nanocrystal [4], and conjugated polymer/TiO_2 [5]. These studies provide fundamental insight into interfacial processes and also assist in designing efficient photovoltaic devices.

Ideally, a composite photovoltaic device should strongly absorb the solar spectrum, exhibit efficient photoinduced charge separation, have slow carrier recombination, and permit efficient charge transport to the electrodes. The Grätzel solar cell [6] employs dye-sensitized semiconductor nanocrystalline thin films as the photoactive layer. In this type of cell, optical excitation of sensitizer molecules such as $Ru(NCS)_2(dcbpy)_2$(Ru N3) leads to efficient charge transfer from sensitizer excited state to semiconductor. A solar-to-electric power conversion efficiency of 10% has been obtained for this system [6]. Using nanocrystalline films rather than nanoparticles is advantageous, as it increases the ability of the semiconductor to transport the charge to the electrode through the connected inorganic network.

Conjugated polymer/inorganic semiconductor nanoporous films have other appealing characteristics. The polymer absorption spectrum and en-

* Corresponding author. Fax: +1-404-727-6586.
E-mail address: tlian@emory.edu (T. Lian).

0009-2614/01/$ - see front matter
PII: S0009-2614(01)01065-X

ergy levels are tunable through functionalization, and charged conjugated polymers can serve as charge-transport materials. The high surface area of the film allows extensive contact between polymer and nanoparticle. A large interface is critical for this system. Conjugated polymers typically have an exciton diffusion radius of 5–15 nm [7,8]. Excitations which occur farther from the interface will likely decay without transferring charge to the inorganic semiconductor, hurting efficiency. Recently, a composite consisting of a nanoporous TiO_2 layer with interpenetrating MEH-PPV as both the photogeneration medium and hole transporter showed good photoconductivity, and promising efficiency [9].

Although charge transfer in conjugated polymer/semiconductor composites has been demonstrated for several systems, very little work has been done to directly study the dynamics of the transfer. For MEH-PPV/TiO_2, the electron transfer is thought to be substantially faster than the rate of polymer exciton decay ($\sim$300 ps) [10], since transfer has been demonstrated and the polymer photoluminescence is quenched [11,12].

Previous work in our group has shown that photoinduced electron transfer can be extremely fast for dyes such as Ru N3 adsorbed onto the surface of nanostructured semiconductors [13,14]. However, there are substantial differences between these systems and composites involving conjugated polymers. Excitons in polymer are delocalized over a few monomer units and the chromophore repeats along the polymer chain. Excitation in the polymer may therefore occur in regions having varying local contact with the nanoparticle. If there is sufficient polymer aggregation, ultrafast interchain electron and Förster energy transfer may also occur [15]. Furthermore, it has been shown that energy may be funneled along a polymer chain depending on its conformation and presence of defect sites [16].

The actual electron transfer from polymer to semiconductor nanoparticle represents an ET process between delocalized donor and acceptor states. This differs from the dye-sensitized system, where ET occurs from the localized molecular excited state to the delocalized semiconductor conduction band. The added complexity provides an exciting and challenging interfacial electron transfer problem, and conjugated polymer/semiconductor composites may serve as an interesting model system to study ET between delocalized donor and acceptor states.

In this work, we present an ultrafast infrared transient absorption study of photoinduced electron transfer from the conjugated polymer MEH-PPV into SnO_2 and TiO_2 nanoporous thin films. The mid-IR absorption signals at the investigated wavelengths originate primarily from electrons injected into the semiconductor film, which allow measurement of the charge separation rate. The long-lived charge separation is confirmed using microsecond time-resolved step-scan FTIR difference spectroscopy.

2. Experimental

Colloidal SnO_2 was synthesized according to a published procedure [17]. The transparent colloidal SnO_2 solution was refluxed for 4 h. 100 ml of this colloid was poured into an autoclave and heated at 150 °C for 1 h, then at 270 °C for 16 h. The solution was then concentrated to 30 ml and 15 drops of TritonX-100 were added. After 1 day stirring, the solution was cast onto sapphire substrates, and dried in air. The thin films were baked at 480–500 °C for 1 h. The samples were then allowed to slowly return to room temperature. Films had good homogeneity and transparency. TiO_2 nanocrystalline films were also prepared according to a published method [18]. The nanoparticles were not capped. Average particle size was $\sim$10 nm for SnO_2, and $\sim$20 nm for TiO_2, obtained from SEM measurements.

MEH-PPV was prepared by the Gilch route [19], similar to that used by Neef and Ferraris [20], which employed the treatment of monomers (α, α'-dibromo-2-methoxy-5-(2-ethylhexyloxy)xylene) with potassium *tert*-butoxide in organic solvents. The TiO_2/MEH-PPV and SnO_2/MEH-PPV films were prepared by soaking the nanoporous films in a 1 mg/10 ml solution of MEH-PPV in chloroform for 2–5 h. The resulting composite films were washed with chloroform and dried in air.

Ultrafast experiments were carried out in a pump–probe transient absorption scheme. The details of the experimental setup have been described previously [21,22]. Briefly, the second harmonic of a regeneratively amplified Ti:Sapphire system (Clark-MXR) at 400 nm was used for excitation. The tunable mid-IR probe beam for these experiments was generated by mixing the signal and idler from an IR-OPA (Clark-MXR) in a $AgGaS_2$ crystal to difference-frequency-generate mid-IR wavelengths tunable from 3–7 μm. The excitation power was ~3 μJ. The pump and the probe beam sizes at the sample were 300 and ~500 μm, respectively. The pulsewidth at the sample was ~200 fs, determined by measuring the signal from a silicon wafer. The sample was constantly moved during data collection. The sample was not noticeably damaged as a result of the laser experiment.

The experimental setup for measurement of microsecond step-scan FTIR spectra has been described elsewhere [23]. The present samples were excited using 532 nm light at 10 Hz, with an excitation power of ~3 mJ, over a spot diameter of ~4 mm.

3. Results and discussion

Ultrafast kinetic traces were collected for MEH-PPV/SnO_2 film using probe energies of 2550, 2000 (shown in Fig. 1), and 1725 cm^{-1}. The dynamics observed at all investigated probe wavelengths were identical within error. A naked film of SnO_2 showed only a slight signal, since SnO_2 has small absorption at 400 nm and low pump power was maintained to avoid multiphoton excitation. Therefore, the MEH-PPV/SnO_2 signal results from processes following absorption of light by the polymer. All the three MEH-PPV/SnO_2 kinetic traces were globally fit using a model convoluting the instrument function with a single exponential absorption increase and a very long-lived decay. The global fit yielded an 800 ± 200 fs timescale for the absorption increase and did not clearly resolve the slight (<5%) decay. Fig. 1 also shows the signal obtained from a silicon wafer to indicate the instrument-response function.

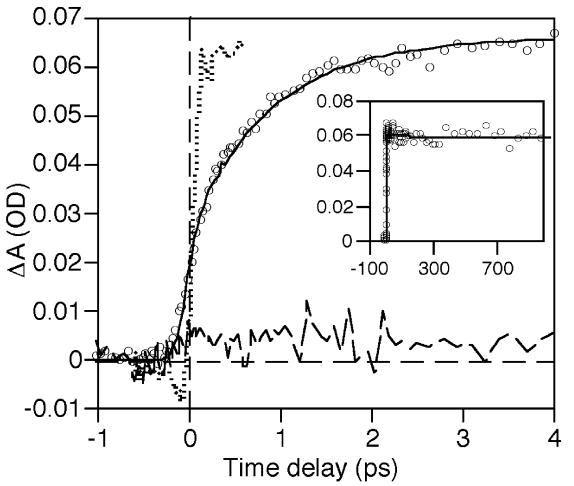

Fig. 1. Transient kinetics measured at 2000 cm^{-1} for MEH-PPV/SnO_2 film (open circles) and SnO_2 naked film (dashed line). The dotted line is the signal from a silicon wafer, included as a reference of the instrument function. The risetime of MEH-PPV/SnO_2 signal was fit using a single exponential with 800 fs timescale. The inset shows the MEH-PPV/SnO_2 signal extending to 1 ns. On this longer timescale, virtually no signal decay is observed.

Fig. 2 shows the femtosecond transient absorption signal for MEH-PPV/TiO_2. It differs substantially from the data for the SnO_2 compos-

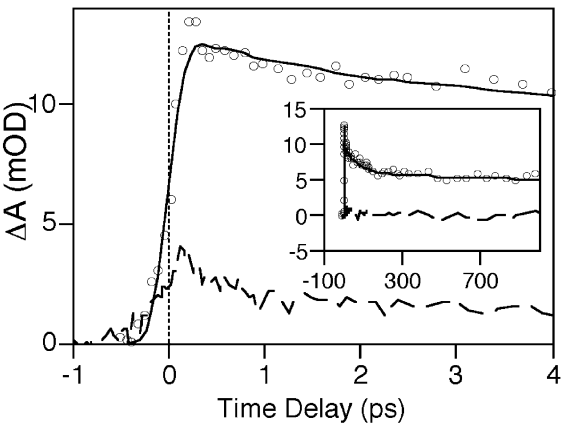

Fig. 2. Open circles show the MEH-PPV/TiO_2 kinetic trace probing at 2000 cm^{-1}. Open triangles show the corresponding data for MEH-PPV/ZrO_2. The inset shows the long-time dynamics. The MEH-PPV/TiO_2 data were fit convoluting the Gaussian instrument function with an instrument-limited (<100 fs) absorption increase, and a three exponential decay with timescales of 2, 75 ps, and infinity.

ite. For MEH-PPV/TiO_2, the absorption signal appears with a timescale <100 fs. Additionally, the signal decays $\sim 50\%$ within 1 ns.

Electron transfer from polymer to nanoparticle is anticipated for both composites. Charge transfer has previously been demonstrated for an MEH-PPV/TiO_2 composite [12]. The polymer excited state lies higher in energy than the TiO_2 conduction band, resulting in favorable energetics for the electron transfer [24,25]. The SnO_2 conduction band lies even lower in energy than that of the TiO_2 [25], so electron transfer from MEH-PPV to SnO_2 is also energetically favorable.

In order to analyze the data presented in Figs. 1 and 2, the origin of the femtosecond mid-IR absorption signal must be discussed. In the composite, several species may contribute to the absorption signal: (1) intrachain MEH-PPV excitons, (2) MEH-PPV polaron pairs formed via interchain charge transfer, (3) MEH-PPV positive polarons generated by electron transfer to SnO_2, (4) electrons injected into SnO_2. Species (1) and (2) are not related to electron transfer from MEH-PPV to SnO_2, while (3) and (4) are products of the charge transfer. See [26] for a review of polymer excitons and polarons.

In a neat MEH-PPV film, an absorption signal with a $\ll 100$ fs risetime has been previously reported probing at 1500 cm^{-1} [27]. We observed similar dynamics probing an MEH-PPV film at 2000 cm^{-1}. The fast-appearing absorption signal has been assigned to polarons formed by interchain electron transfer, which is possible when the polymer molecules are in close contact, as in a film [27]. However, polaron formation via interchain charge transfer is strongly inhibited when polymer chains are dispersed [28]. In the nanoporous film composites, the polymer molecules are somewhat dispersed due to the irregular surface. However, some interchain transfer may still be possible, which would contribute to the observed signal.

As a control experiment, an MEH-PPV/ZrO_2 film was prepared with similar polymer concentration as MEH-PPV/TiO_2, and studied under identical conditions. ZrO_2 was chosen because it has a higher-lying conduction band, which prevents electron transfer from MEH-PPV [12]. The trace is shown in Fig. 2. A small absorption signal is observed, with a fast rise, and decay dynamics that qualitatively agree with those of [27] and our neat MEH-PPV film probed at 2000 cm^{-1}. However, the MEH-PPV film signal was more than five times larger, which can be attributed to the increased contact between chains.

MEH-PPV intrachain excitons are not significant contributors to the observed IR signals. The excitons have a 200–300 ps lifetime at room temperature [10]. However, the MEH-PPV/SnO_2 mid-IR absorption remains nearly constant for at least 1 ns, and MEH-PPV/TiO_2 also exhibits slower decay dynamics. Furthermore, excitation of MEH-PPV/ZrO_2 should form an abundance of excitons, yet its mid-IR signal was quite small and exhibited dynamics which agreed with the polaron signal seen in MEH-PPV film and Ref. [27].

The absorption signals from MEH-PPV/TiO_2 and MEH-PPV/SnO_2 are therefore dominated by electron transfer from polymer to nanoparticle, although they may contain a small contribution from interchain transfer. Transfer from polymer to nanoparticle forms an MEH-PPV positive polaron and an electron injected into the semiconductor nanoporous film. MEH-PPV positive polarons have a broad subgap absorption band centered at 0.53 eV (~ 4300 cm^{-1}), which extends below 2500 cm^{-1} [12]. Electrons injected into a semiconductor conduction band also exhibit a very broad absorption in the mid-IR. Our group has frequently used this absorption to study photoinduced electron transfer for molecular dye/nanostructured semiconductor systems [14,29,35]. Although two species may be responsible for the signal shown in Fig. 1, both are products of the electron transfer from polymer to inorganic semiconductor. Therefore, the risetime of the mid-IR absorption in these composites corresponds to the timescale of photoinduced electron transfer. This transfer is subpicosecond for both samples. Electron transfer in these composites can be as fast, or even faster than the transfer from a molecular dye chemisorbed to the colloid surface [14]. The origin of the differences in risetime and decay of the MEH-PPV/SnO_2 and MEH-PPV/TiO_2 signals will be discussed below.

Time-resolved step-scan FTIR difference spectroscopy with 5 μs time resolution was used to

verify photoinduced charge separation and clarify the spectra of the polaron and injected electron. The 50 μs spectrum for MEH-PPV/TiO_2 is shown in Fig. 3. A broad absorption band is seen at ~4300 cm^{-1}. This coincides with the MEH-PPV polaron subgap absorption band [12]. Narrower bands are also present at ~1500 cm^{-1}, and <1200 cm^{-1}. These lower-energy bands have been observed following photoinduced electron transfer from MEH-PPV to C_{60} [30]. They arise from infrared active vibrations (IRAV), in which Raman-active modes become IR-active due to the presence of a charged defect on the chain (i.e., a polaron) [31]. These bands may be used as a probe of the charge carrier density, and their presence further confirms long-lived photoinduced charge separation. The microsecond kinetic trace for the 4300 cm^{-1} absorption band is shown in Fig. 4. The IRAV bands showed identical decay dynamics. Substantial decay is observed, but some charge separation persists well beyond 1 ms for MEH-PPV/TiO_2.

As discussed earlier, the IR signal may arise from both MEH-PPV positive polarons and injected electrons. However, only the polaron signal is clearly resolved in the MEH-PPV/TiO_2 data. To explore this, the spectrum of a Ru N3-sensitized

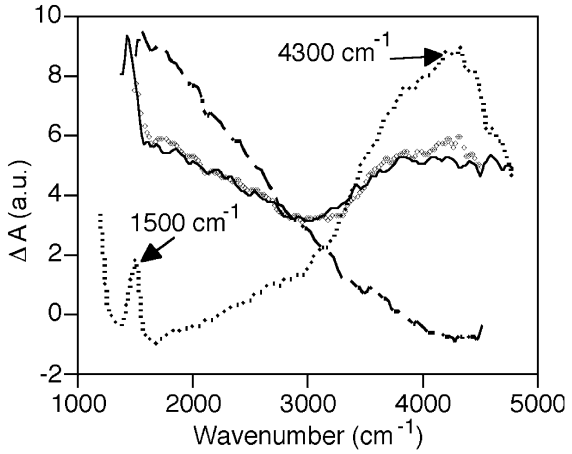

Fig. 3. Step-scan spectra collected at 50 μs for MEH-PPV/SnO_2 (solid line), Ru N3/SnO_2 (dashed line), and MEH-PPV/TiO_2 (dotted line). The symbols represent the fit to the MEH-PPV/SnO_2 spectrum from a scaled sum of the Ru N3/SnO_2 and MEH-PPV/TiO_2 signals.

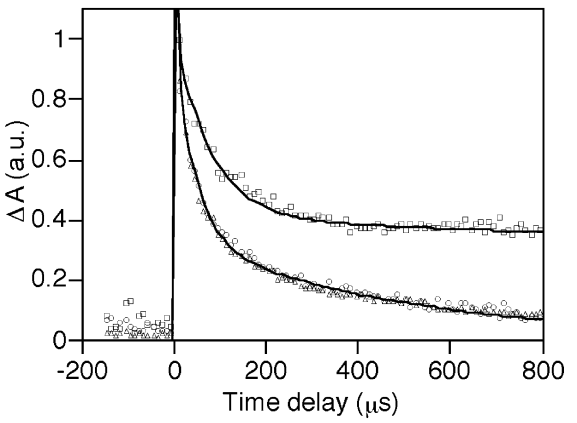

Fig. 4. Normalized microsecond kinetic traces for MEH-PPV/TiO_2 positive polaron band (open squares), MEH-PPV/SnO_2 polaron band observed at ~4300 cm^{-1} (open circles), and MEH-PPV/SnO_2 injected electron absorption observed at 2100 cm^{-1} (open triangles). The MEH-PPV/TiO_2 trace fits using exponential components with timescales of 3, 80 μs, and infinity. Both MEH-PPV/SnO_2 traces are fit using exponential components of 3, 44, and 500 μs.

TiO_2 film was also collected. Charge recombination in an unbiased Ru N3/TiO_2 system occurs on the μs–ms timescale [32]. However, the step-scan spectrum again showed no clear evidence of the TiO_2 electron signal. The failure to observe the injected electron is therefore due to decay of the electron absorption cross-section. Rapid cross-section decay due to electron trapping has been observed in colloidal TiO_2 particles [33] and thin films [34].

The 50 μs MEH-PPV/SnO_2 spectrum is also shown in Fig. 3. It exhibits two broad absorption bands. The higher-energy band is suggestive of the polaron electronic transition seen in MEH-PPV/TiO_2 above. Additionally, the narrow IRAV peak at 1500 cm^{-1} is evident, clearly indicating charge separation. The second broad absorption increases toward lower-energy probe, and exhibits no clear peak. The spectrum of a Ru N3-sensitized SnO_2 film is shown in Fig. 3. In contrast to Ru N3/TiO_2, this sample shows a broad absorption, gradually rising toward longer wavelength. This corresponds to the electron injected into SnO_2.

Therefore, the MEH-PPV/TiO_2 spectrum corresponds to the MEH-PPV positive polaron, and the Ru N3/SnO_2 signal corresponds to the electron

injected into SnO_2. Charge transfer in MEH-PPV/SnO_2 results in formation of both species. As anticipated, the MEH-PPV/SnO_2 spectrum is well reproduced by a scaled sum of the two components (shown in Fig. 3). The kinetic traces for the two bands are shown in Fig. 4. Both exhibit identical dynamics, indicating that the decay is exclusively carrier recombination, and there is no electron cross-section decay on this timescale. The microsecond recombination dynamics are faster than those of MEH-PPV/TiO_2, with recombination virtually complete within 1 ms.

The differences in the ultrafast dynamics of the two composites may now be discussed. The MEH-PPV/TiO_2 signal decayed ~50% within 1 ns, while the MEH-PPV/SnO_2 signal showed no significant decay. Based on the step-scan experiments, the polaron does not strongly contribute to the transient absorption at the ultrafast probe wavelengths. Therefore, the signals arise primarily from the injected electron. Since the electron cross-section decay in TiO_2 is much faster than in SnO_2, the early decay seen in MEH-PPV/TiO_2 may be attributable to electron trapping rather than fast carrier recombination. This issue will be addressed in a future study.

An interesting feature of both MEH-PPV composites is the lack of evidence for multiple injection timescales from excitons that diffuse varying distances to the interface prior to injection. Signal from this process could be masked in the present data by electron cross-section decay. Future work will address the extent of slow injection in these systems. Nevertheless, it is clear that the majority of charge transfer in both composites occurs within ~1 ps. The large interface of the composite minimizes the necessity for exciton diffusion. This indicates that charge transfer can be quite fast and efficient in polymer/nanoporous semiconductor film composites assuming favorable energetics and a large interface.

Although SnO_2 has a lower-lying conduction band than TiO_2, it exhibits slower electron injection. The relative energy of the polymer exciton compared with the semiconductor conduction band is therefore not the only factor affecting injection rate. It is possible that this difference is a result of different film morphology between the two semiconductors. However, slower injection to SnO_2 has been observed for molecular dye-sensitized semiconductors as well [35]. The reason for this is still being studied, and may relate to the differences between the conduction band of SnO_2, which is of s orbital character, and TiO_2, which is of d orbital character. This affects coupling, and also the density of accepting states in the semiconductor conduction band.

4. Conclusions

We have demonstrated subpicosecond photoinduced electron transfer from the conjugated polymer MEH-PPV to SnO_2 and TiO_2 nanoporous thin films. The large interface between the two materials and favorable energetics facilitate the ultrafast charge transfer, minimizing the need for exciton diffusion to the interface. Although the MEH-PPV is physisorbed rather than chemisorbed to the surface, the observed electron transfer rate is extremely fast. The slower injection rate for SnO_2 despite a lower-lying conduction band indicates that energetics are not the only factor determining the injection rate. Morphology of the composite and the nature of the semiconductor conduction band are also important factors in the rate and efficiency of the charge transfer.

MEH-PPV/SnO_2 exhibited virtually no carrier recombination within 1 ns. MEH-PPV/TiO_2 shows significant signal decay within 1 ns, although this may arise from electron trapping in the TiO_2, rather than carrier recombination. Both composites show a large decay in charge separation on the microsecond timescale, although some carriers in MEH-PPV/TiO_2 persist for several seconds. The ability to easily prepare composites which undergo fast charge separation and slow recombination show that conjugated polymer/inorganic semiconductor nanoporous film composites hold promise for photovoltaic applications.

Acknowledgements

This work is supported by the National Science Foundation CAREER award under grant No.

9733796. We also would like to acknowledge the partial financial support by the Petroleum Research Fund, administered by the ACS and the Emory University Research Committee. G.H. acknowledges support from a research initiation grant and quality improvement funds from Georgia State University.

References

[1] A.P. Alivasatos, Science 271 (1996) 933.
[2] N.C. Greenham, R.H. Friend, Solid State Phys. 49 (1995).
[3] N.S. Sariciftci, L. Smilowitz, A.J. Heeger, F. Wudl, Science 258 (1992) 1474.
[4] N.C. Greenham, X. Peng, A.P. Alivasatos, Phys. Rev. B 54 (1996) 17628.
[5] M.P.T. Christiaans, M.M. Wienk, P.A. van Hal, J.M. Kroon, R.A.J. Janssen, Synth. Met. 101 (1999) 265.
[6] B. O'Regan, M. Grätzel, Nature 335 (1991) 737.
[7] J.J.M. Halls, K. Pichler, R.H. Friend, S.C. Moratti, A.B. Holmes, Appl. Phys. Lett. 68 (1996) 3120.
[8] P.J. Hamer, K. Pichler, M.G. Harrison, R.H. Friend, B. Ratier, A. Moliton, S.C. Moratti, A.B. Holmes, Philos. Mag. A 73 (1996) 367.
[9] A.C. Arango, S.A. Carter, Appl. Phys. Lett. 74 (1999) 1698.
[10] L. Smilowitz, A. Hays, A.J. Heeger, G. Wang, J.E. Bowers, J. Chem. Phys. 98 (1993) 6504.
[11] T.J. Savenije, J.M. Warman, A. Goossens, Chem. Phys. Lett. 287 (1998) 148.
[12] P.A. van Hal, M.P.T. Christiaans, M.M. Wienk, J.M. Kroon, R.A.J. Janssen, J. Phys. Chem. B 103 (1999) 4352.
[13] R.J. Ellingson, J.B. Asbury, S. Ferrere, H.N. Ghosh, J.R. Sprague, T. Lian, A.J. Nozik, J. Phys. Chem. B 102 (1998) 6455.
[14] J.B. Asbury, R.J. Ellingson, H.N. Ghosh, S. Ferrere, A.J. Nozik, T. Lian, J. Phys. Chem. B 103 (1999) 3110.
[15] T.-Q. Nguyen, J. Wu, V. Doan, B.J. Schwartz, S.H. Tolbert, Science 288 (2000) 652.
[16] D.A. Vanden Bout, W.-T. Yip, D. Hu, D.-K. Fu, T.M. Swager, P.F. Barbara, Science 277 (1997) 1074.
[17] T. Nutz, U.Z. Felde, M. Haase, J. Chem. Phys. 110 (1999) 12142.
[18] A. Zaban, S. Ferrere, J.R. Sprague, B.A. Gregg, J. Phys. Chem. B 101 (1997) 55.
[19] H.G. Gilch, W.L. Wheelwright, Polym. Sci., Part A 4 (1966) 1337.
[20] C.J. Neef, J.P. Ferraris, Macromolecules 33 (2000) 2311.
[21] H.N. Ghosh, J.B. Asbury, T. Lian, J. Phys. Chem. B 102 (1998) 6482.
[22] Y.Q. Wang, J.B. Asbury, T. Lian, J. Phys. Chem. B 104 (2000) 4291.
[23] G. Hastings, Appl. Spectrosc. 55 (2001) 894.
[24] M.M. Richter, F.R.F. Fan, F. Klavetter, A.J. Heeger, Chem. Phys. Lett. 226 (1994) 115.
[25] A. Hagfeldt, M. Grätzel, Chem. Rev. 95 (1995) 49.
[26] P.A. Lane, Z.V. Vardeny, in: P.C. Ekland, A.M. Rao (Eds.), Fullerene Polymers and Fullerene Polymer Composites, Springer, Berlin, 2000, p. 69.
[27] D. Moses, A. Dogariu, A.J. Heeger, Chem. Phys. Lett. 316 (2000) 356.
[28] M. Yan, L.J. Rothberg, E.W. Kwock, T.M. Miller, Phys. Rev. Lett. 75 (1995) 1992.
[29] J.B. Asbury, E. Hao, Y.Q. Wang, T. Lian, J. Phys. Chem. B 104 (2000) 11957.
[30] U. Mizrahi, I. Shtrichman, D. Gershoni, E. Ehrenfreund, Z.V. Vardeny, Synth. Met. 102 (1999) 1182.
[31] E. Ehrenfreund, Z.V. Vardeny, Proc. SPIE-Int. Soc. Opt. Eng. 3145 (1997) 324.
[32] S.A. Haque, Y. Tachibana, R.L. Willis, J.E. Moser, M. Grätzel, D.R. Klug, J.R. Durrant, J. Phys. Chem. B 104 (2000) 538.
[33] H.N. Ghosh, J.B. Asbury, Y. Weng, T. Lian, J. Phys. Chem. B 102 (1998) 10208.
[34] J.B. Asbury, E. Hao, T. Lian, unpublished.
[35] J.B. Asbury, E. Hao, Y.Q. Wang, H.N. Ghosh, T. Lian, J. Phys. Chem. B 105 (2001) 4545.